STRUCTURAL ANALYSIS OF HELICAL BIMETALLIC STRIP THERMOSTAT

Dănuț Zahariea[1]

[1] "Gheorghe Asachi" Technical University of Iasi-Romania, Department of Fluid Mechanics, Hydraulic Machines and Drives, Blvd. D. Mangeron, No. 59A, 700050, Iasi, Romania

Corresponding author: Dănuț Zahariea, dzahariea@tuiasi.ro

Abstract: In this paper the structural analysis of a helical bimetallic strip thermostat will be analyzed using CATIA Generative Structural Analysis workbench. Regarding the materials, six different helical bimetallic strips will be considered, with titanium as passive layer and zinc, aluminium, bronze, brass, cooper and steel as active layer. The structural analysis procedure will be presented: 3D model generation; mesh definition; restraints, loads and interaction conditions; analysis and results visualization. The numerical analysis will be performed under the same general condition (geometrical characteristics, restraints and thermal load) but using two variable parameters: the number of turns and the strips width. For all these study cases analyzed only the thermal load generated by an external temperature field will be considered. A certain combination of materials (titanium-zinc) will be fully presented.

Key words: thermostat, helical bimetallic strip, structural analysis, CATIA.

1. INTRODUCTION

The controlling process of the systems temperature can be mabe by using thermostats. One of the most common thermostat has a bimetallic strip like temperature sensitive device. The bimetallic strip is composed by two strips bounded together by brazing or welding. The strips are made of different materials (active and passive) having different coefficients of thermal expansion α_a and α_p ($\alpha_a > \alpha_p$). As long as the difference $\alpha_a - \alpha_p$ between these two coefficients of thermal expansion is increasing, the bending of the bimetallic strip under the same temperature will be higher, thus the sensitivity of the temperature sensitive device will increase as well. The sensitivity increasing can also be obtained by changing some geometric characteristics, for example decreasing the thickness or increasing the length. The terminology, the properties for selected materials used in bimaterial temperature elements and the basic equations are presented in (Sandberg, 2000). The more complex calculating formulae with examples of calculation for different configurations (cantilever strip, simple beam, U-shape, spiral and helical coils, etc.), the industrial applications, as well as some industrial products with geometric and functional characteristics are presented in (Kanthal, 2008).

In (Zahariea & Stachie, 2010) the straight bimetallic strip has been investigated using the 3D finite element analysis.

This paper is devoted to a 3D finite element analysis based investigation using the CATIA Generative Structural Analysis workbench (Zamani, 2005 and Ghionea, 2007) of another important constructive solution: the helical bimetallic strip. The helical bimetallic strip to be analyzed is presented in figure 1. The geometric characteristics of the two layers of the helical bimetallic strip are presented in figure 2 (for active layer) and figure 3 (for passive layer).

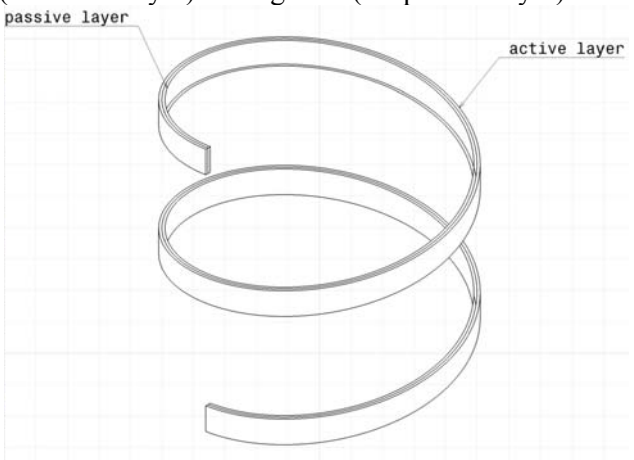

Fig. 1. The helical bimetallic strip, p=50 mm

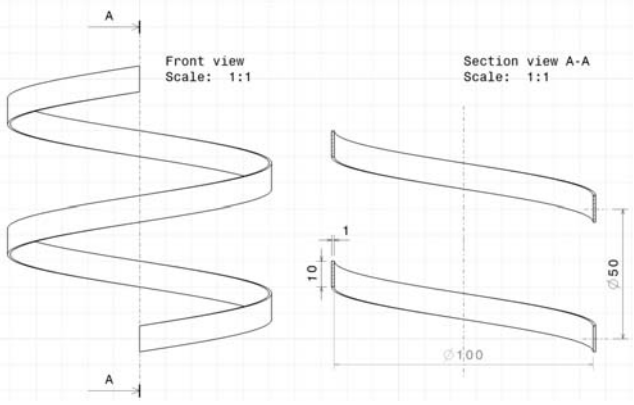

Fig. 2. The geometric characteristics of the active layer

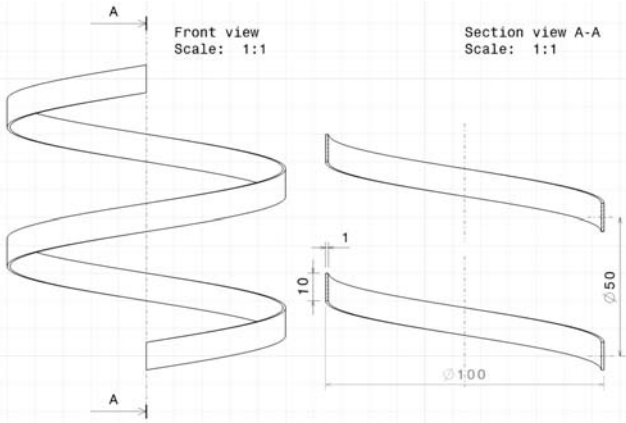

Fig. 3. The geometric characteristics of the passive layer

For both helical layers, a generative circular helix has been considered (figure 4). The geometric parameters of the generative circular helix are: the radius R=50 mm, the pitch p=50 mm, the total height H=100 mm, the circular helix orientation is counterclockwise.

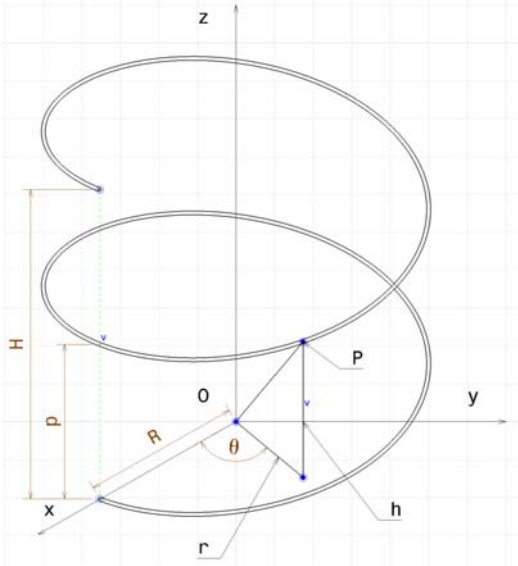

Fig. 4. The geometric characteristics of the generative helix

The generative helix is a curve in 3-dimensional space and can be described by the following parametrisation:

$$x(t)=R\cdot\cos(t);\ y(t)=R\cdot\sin(t);z(t)=p/(2\pi)\cdot t \qquad (1)$$

where the parameter $t\in[0,T]$, with the winding angle $T=2\pi H/p$.
The length of the circular helix can be expressed by the following relationship:

$$L=T\cdot\{R^2+[p/(2\cdot\pi)]^2\}^{0.5} \qquad (2)$$

A better analysis development can be performed if the carthezian (x,y,z) system of coordinates will be replaced with a cylindrical (r,θ,h) system of coordinates. Thus, the circular helix parametrisation becomes:

$$r(t)=R;\ \theta(t)=t;\ h(t)=p/(2\pi)\cdot t \qquad (3)$$

Two other helical bimetallic strips will be analized, having the same values of the geometric parameters like the first one, except the pitch, which will be 25mm (figure 5), and 12.5 mm (figure 6).

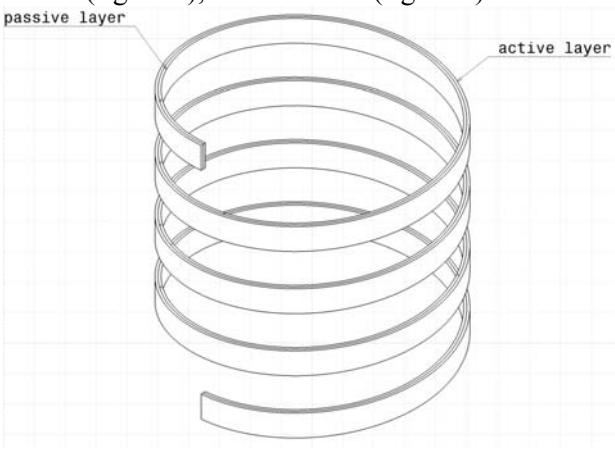

Fig. 5. The helical bimetallic strip, p=25 mm

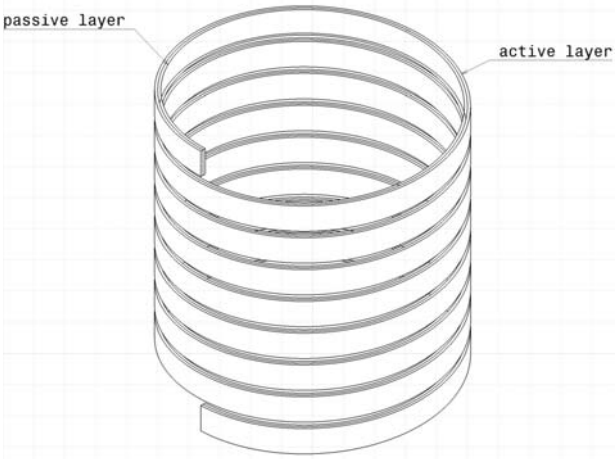

Fig. 6. The helical bimetallic strip, p=12.5 mm

The variable global geometric characteristics for the generative circular helix are summarized in table 1.

Table 1. Global geometric characteristics

	Radius, R [mm]	Height, H [mm]	Pitch p [mm]	Winding angle, T [rad]	Length, L [mm]
1.	50	100	50	4π	636.2
2.			25	8π	1260.6
3.			12.5	16π	2515.3

The material used for passive layer is titanium (pm). As for the active layer, six different materials will be used: zinc (am_1), aluminium (am_2), bronze (am_3), brass (am_4), copper (am_5) and steel (am_6). The most important material characteristics, from the point of view of the structural analysis, are shown in table 2.

Table 2. Material characteristics

	pm	am_1	am_2	am_3	am_4	am_5	am_6
$E\cdot10^{11}$ [Pa]	1.14	0.97	0.7	1.1	1.31	1.1	2
$\alpha\cdot10^{-6}$ [°C^{-1}]	9.5	31.2	23.6	17.8	16.7	16.5	11.7
σ_{02} [MPa]	825	140	95	520	350	290	250

In (Kanthal, 2008) has been noticed that the bimetallic strip will bend in the length direction but also in the width direction, this double curvature

explaining the difference between the measured and the theoretical length curvatures. According to the results presented in this paper, this length curvature difference could be explained also by the helical shape deformation of the bimaterial strip, thus from the initial circular helix, through deformation generated by the external temperature field, the global helical shape will becomes a conical helix.
The structural analysis performed in this paper, will be developed according to a procedure which the main steps are: creating the 3D model; creating the 3D finite element model; applying the restraints and the loads; applying the interaction conditions between the active layer and the passive layer; running the numerical analysis and the results visualization. As for the results, the graphic representation of the von Misses stress distribution, the displacements and the deformed mesh will be analysed. Also, a comparative study of the influence of the mesh type on the global error rate will be presented.
Further investigations should be made on the temperature sensitive devices, based on the helical bimetallic strip, with more complex geometry, for example the temperature sensitive device composed by two helical bimetallic strips with generative radii R_1 and R_2 ($R_2<R_1$), one inside the other.

2. STRUCTURAL ANALYSIS

2.1. The finite element model

In order to obtain the finite element model the tetrahedral elements will be used of both types: linear and parabolic. For the same 3D model, different finite element models can be obtained changing the characteristic parameters: the size and the sag. There are several methods used to change the mesh parameters: the global method; the local method and the adaptive method. In order to select the best finite element model the global error rate criterion ($\varepsilon_{cr}\approx10\%$) will be used.
For helical bimetallic strip with p=50 mm, using the global method of the mesh definition with the following values: size=7.5 mm and sag=1.2 mm, for the mesh obtained with linear finite elements (1206 nodes and 2866 elements) the global error rate is ε_l=24.17%, and for the mesh obtained with parabolic finite elements (6102 nodes and 3512 elements) the global error rate is ε_p=20.81%. The deformed mesh obtained with the global method of mesh definition is presented in figure 7.
The deformation of the 3D finite element model will take place after all the three cylindrical coordinates (r,θ,h), but for the helical bimetallic strip, the most important deformation will take place after the θ cylindrical axis.
In figure 8 the displacements of the finite element model only for θ cylindrical axis direction using the arrows technique are presented.

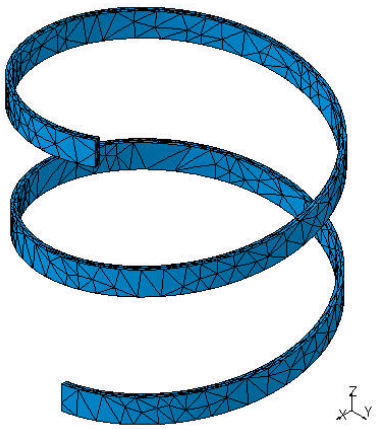

Fig. 7. The deformed mesh by global method, p=50mm.

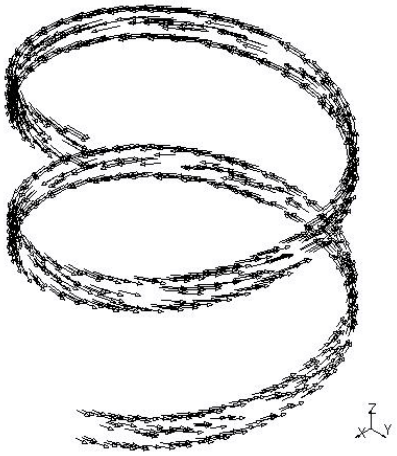

Fig. 8. The displacements after the θ axis, p=50 mm

In order to achieve the global error rate imposed, the mesh must be improved. The adaptive method has been used with an objective global error rate of 14%.
The improved mesh obtained with parabolic finite elements (17405 nodes and 10649 elements) allows the obtaining of a global error rate of 8.34%. The improved deformed mesh is presented in figure 9.

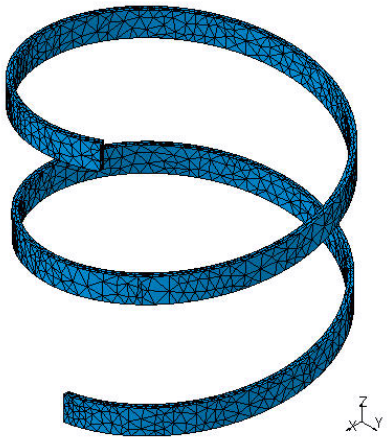

Fig. 9. The improved deformed mesh by adaptive method, p=50 mm

For helical bimetallic strip with p=25 mm the same level of the global error rate ($\varepsilon\approx10\%$) for selecting the best finite element model has been used. Using the

global method of mesh definition with the following values: size=7.5mm and sag=1.2 mm, for the mesh obtained with linear finite elements (2423 nodes and 5913 elements) the global error rate is ε_l=23.63% and for the mesh obtained with parabolic finite elements (12403 nodes and 7202 elements) the global error rate is ε_p=20.74%. The deformed mesh is presented in figure 10.

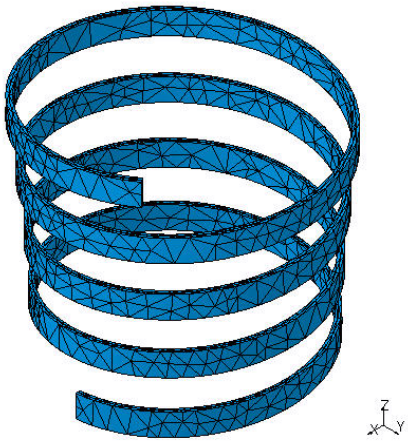

Fig. 10. The deformed mesh by global method, p=25 mm

In order to achieve the global error rate imposed, the mesh must be improved. The adaptive method has been used with an objective global error rate of 14%. The improved mesh obtained with parabolic finite elements (36279 nodes and 22448 elements) allows the obtaining of a global error rate of 7.85%. The improved deformed mesh is presented in figure 11.

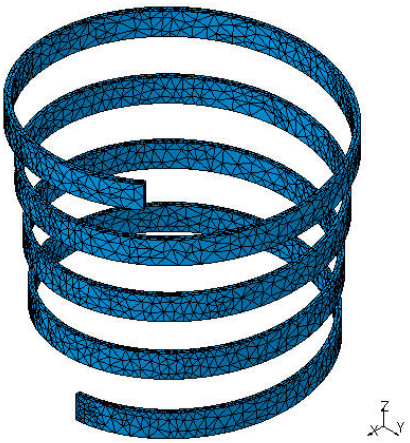

Fig. 11. The improved deformed mesh by adaptive method, p=25 mm

For helical bimetallic strip with p=12.5 mm the same level of the global error rate ($\varepsilon \approx 10\%$) for selecting the best finite element model has been used. Using the global method of mesh definition with the following values: size=7.5mm and sag=1.2 mm, for the mesh obtained with linear finite elements (4793 nodes and 11703 elements) the global error rate is ε_l=22.64% and for the mesh obtained with parabolic finite elements (24562 nodes and 14218 elements) the global error rate is ε_p=20.12%. The deformed mesh is presented in figure 12.

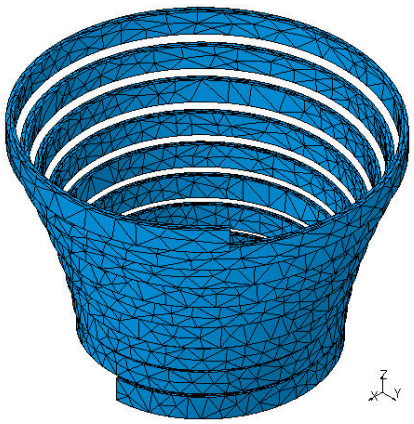

Fig. 12. The deformed mesh by global method, p=12.5 mm

In order to achieve the global error rate imposed, the mesh must be improved. The adaptive method has been used with an objective global error rate of 14%. The improved mesh obtained with parabolic finite elements (75621 nodes and 46617 elements) allows the obtaining of a global error rate of 7.61%. The improved deformed mesh is presented in figure 13.

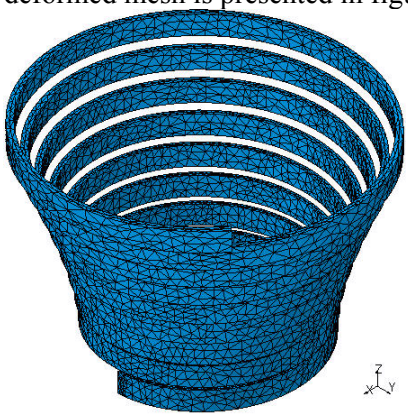

Fig. 13. The improved deformed mesh by adaptive method, p=12.5 mm

2.2. The restraints, the loads and the interaction condition

On the bottom end of both active and passive layers a clamp restraint has been applied. The temperature field, t=50°C, has been applied on both elements of the bimetallic sensitive device. The fastened connection property has been used between the corresponding surfaces on both active and passive layers. In figure 14 the 3D model with restraints, loads and interaction condition is presented.

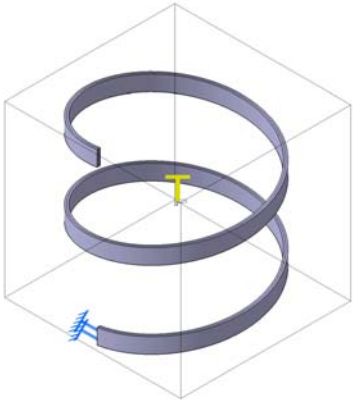

Fig. 14. The restraints, the loads and the interaction conditions

2.3. The analysis results for p=50 mm

The displacements for both elements of the helical bimetallic strip are presented in figure 15. The von Misses stresses for both active and passive layers are presented in figure 16. The von Misses stresses only for the active layer are presented in figure 17. The von Misses stresses only for the passive layer are presented in figure 18.

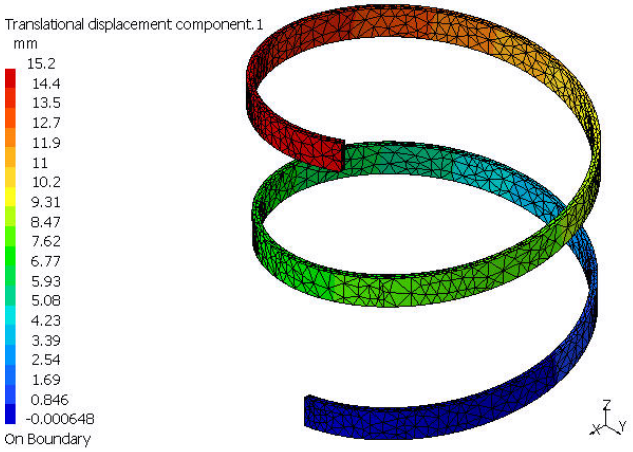

Fig. 15. The displacements, p=50 mm

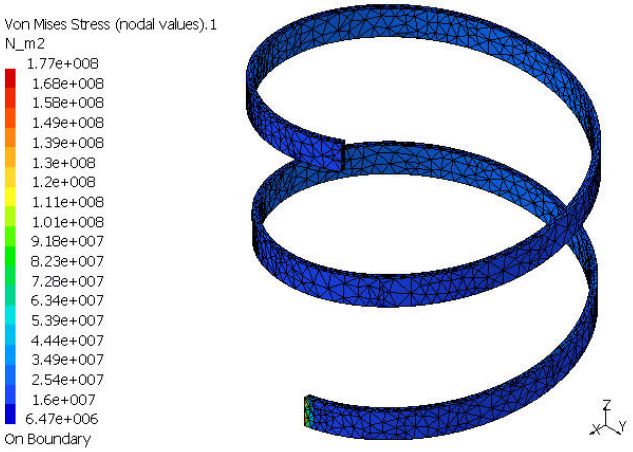

Fig. 16. The von Mises stress for both active and passive layers, p=50 mm

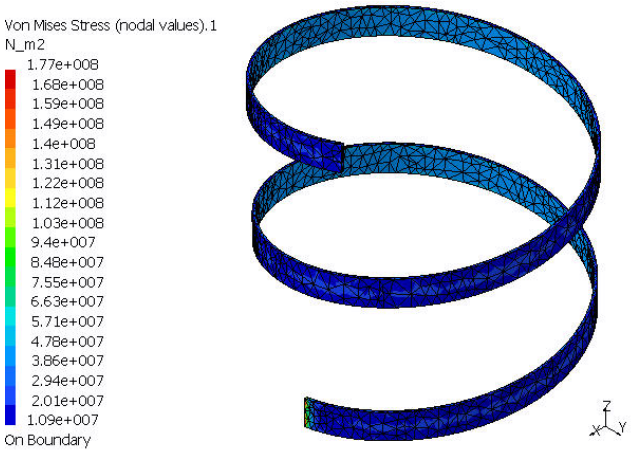

Fig. 17. The von Mises stress for the active layer, p=50 mm

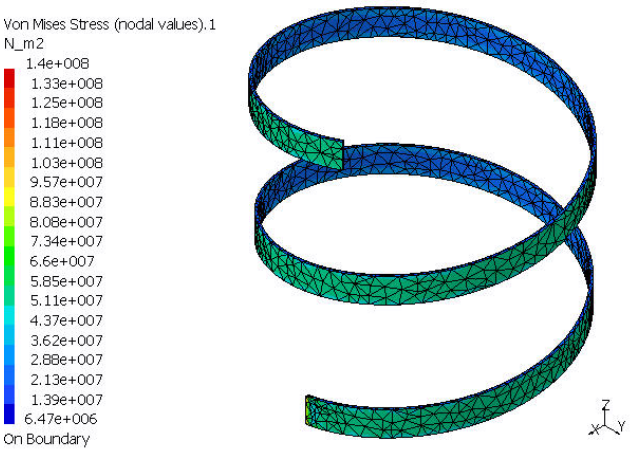

Fig. 18. The von Mises stress for the passive layer, p=50 mm

2.4. The analysis results for p=25 mm

The displacements for both elements of the helical bimetallic strip are presented in figure 19. The von Misses stresses for both active and passive layers are presented in figure 20. The von Misses stresses only for the active layer are presented in figure 21. The von Misses stresses only for the passive layer are presented in figure 22.

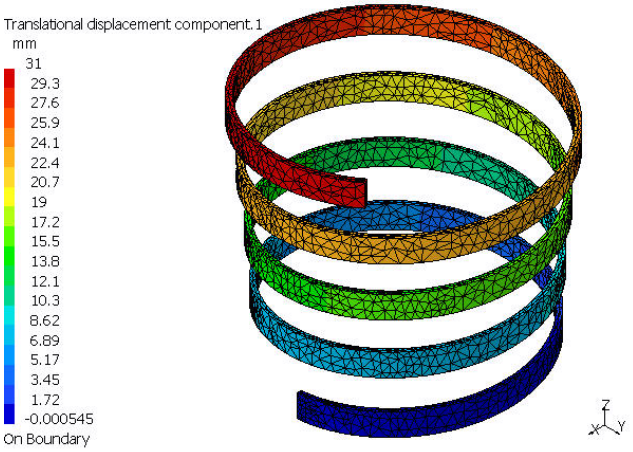

Fig. 19. The displacements, p=25 mm

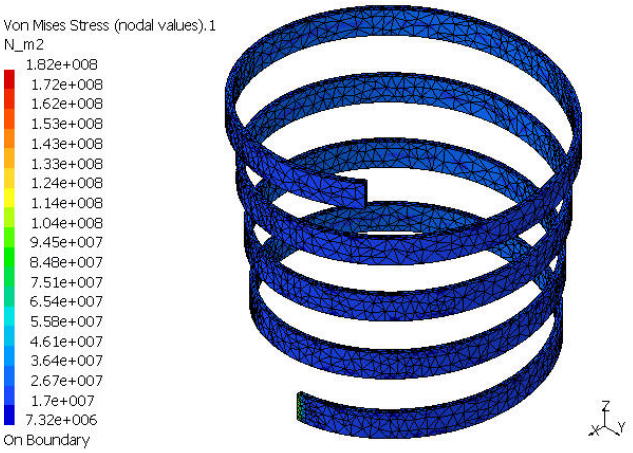

Fig. 20. The von Mises stress for both active and passive layers, p=25 mm

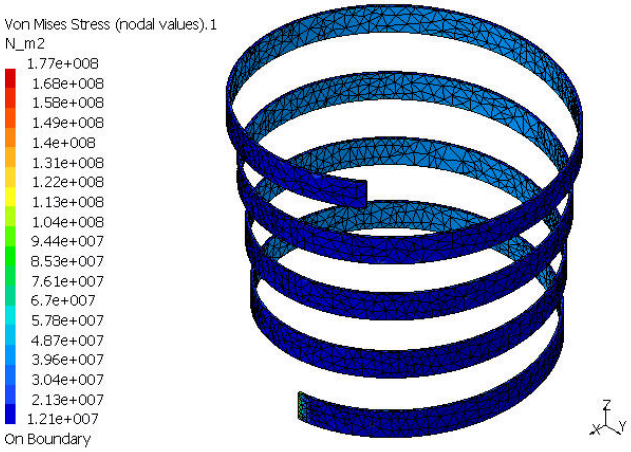

Fig. 21. The von Mises stress for the active layer, p=25 mm

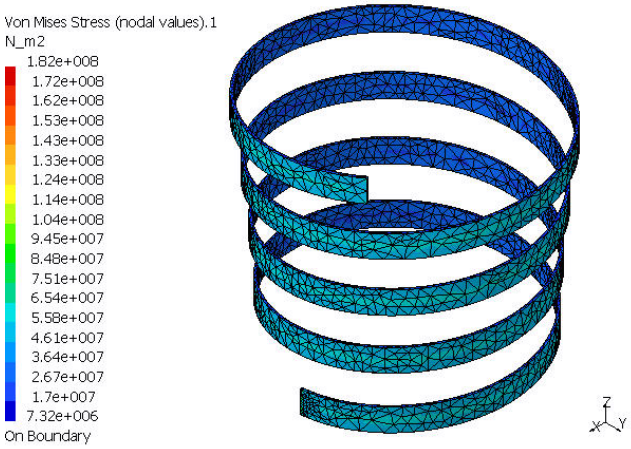

Fig. 22. The von Mises stress for the passive layer, p=25 mm

2.5. The analysis results for p=12.5 mm

The displacements for both elements of the helical bimetallic strip are presented in figure 23. The von Misses stresses for both active and passive layers are presented in figure 24. The von Misses stresses only for the active layer are presented in figure 25. The von Misses stresses only for the passive layer are presented in figure 26.

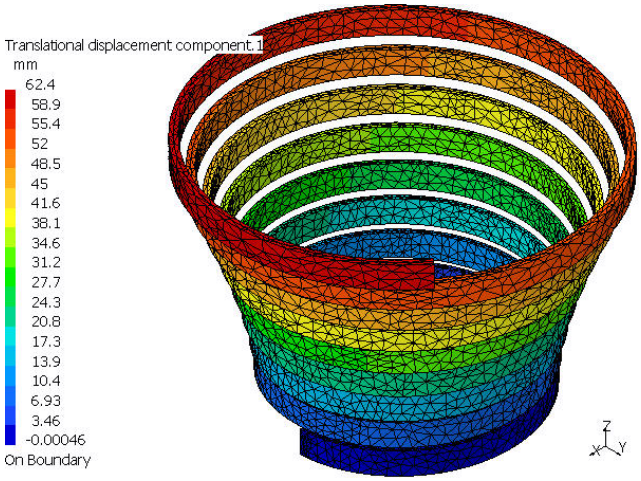

Fig. 23. The displacements, p=12.5 mm

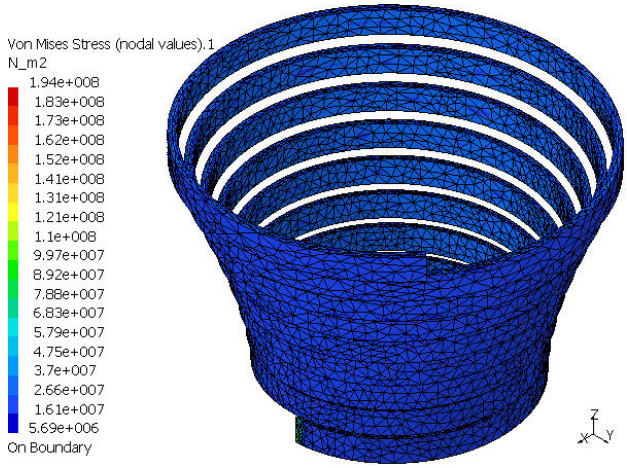

Fig. 24. The von Mises stress for both active and passive layers, p=12.5 mm

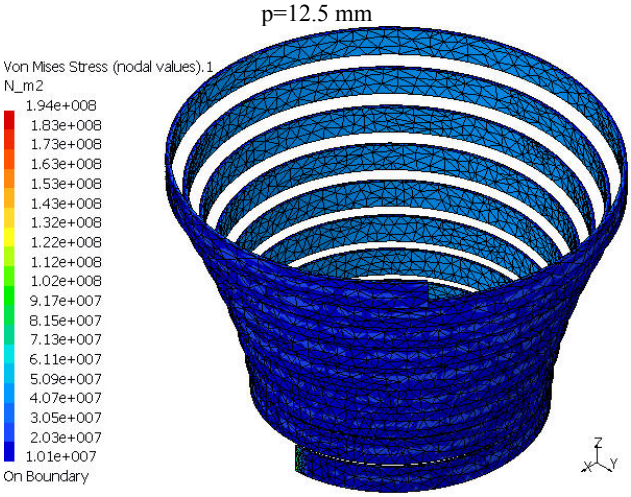

Fig. 25. The von Mises stress for the active layer, p=12.5 mm

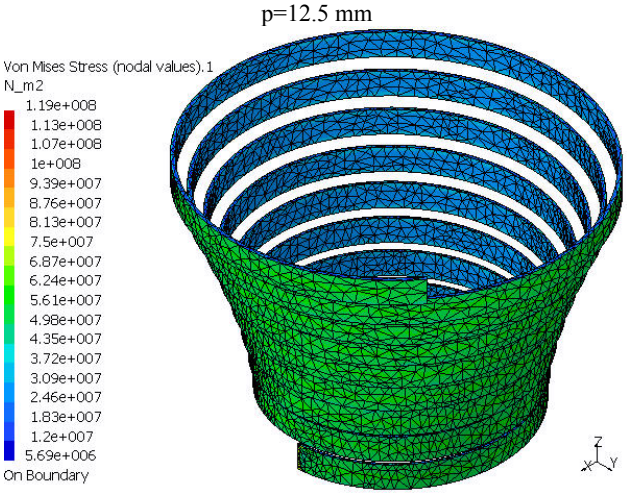

Fig. 26. The von Mises stress for the passive layer, p=12.5 mm

3. COMPARATIVE ANALYSIS

Two comparative analyses will be performed. First one is studying the influence of the strips width b={6, 8, 10} mm for the same helical winding angle T=16π (which coressponds to the pitch p=12.5 mm). The second one is studying the influence of the helical winding angle T={4π, 8π, 16π} (which corresponds to the pitch p={50, 25, 12.5}mm) for the same strips width b=10 mm. The thickness for both active and passive layer is equal to 1 mm.

3.1. The influence of the strips width

For every combination of materials, the strips width has been changed (b={6, 8, 10} mm), while the helical winding angle has been maintained constant (T=16π which corresponds to a helix with 8 turns). The numerical values for maximum deflection (ΔL [mm]), for the von Misses stress on the active layer (σ_{ea} [MPa]), as well as for the passive layer (σ_{ep} [MPa]), are presented in figures 27, 28, 29.

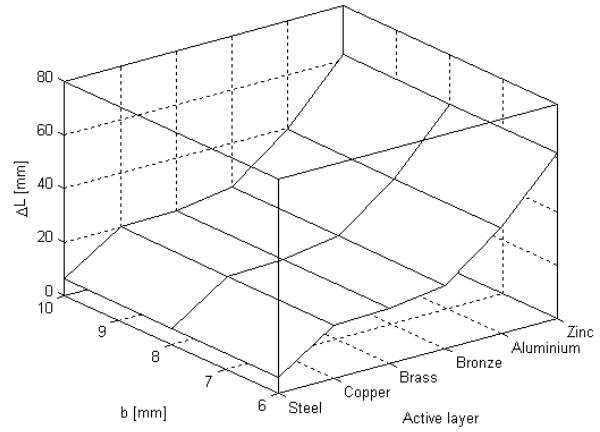

Fig. 27. The influence of the strips width on the maximum deflection

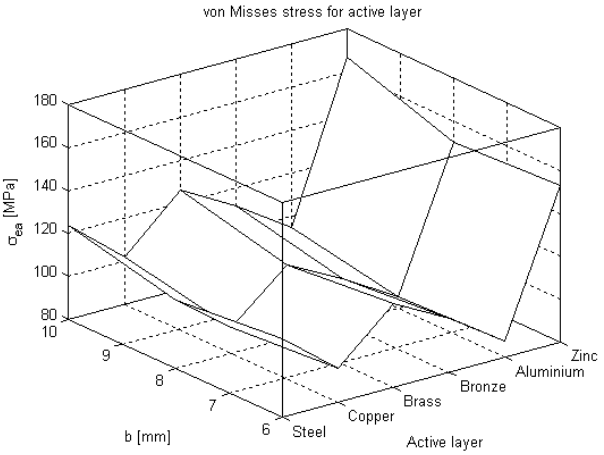

Fig. 28. The influence of the strips width on the von Misses stress for active layer

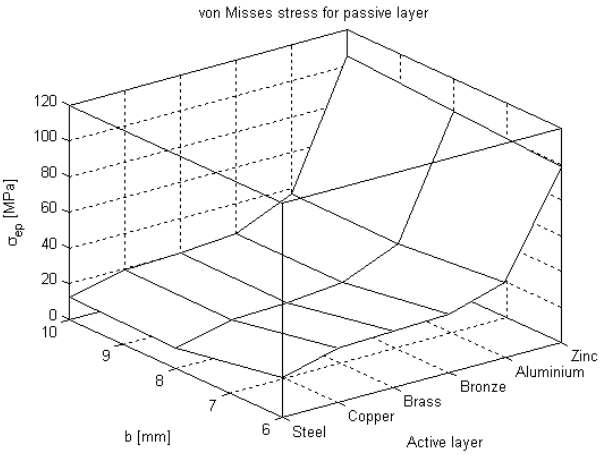

Fig. 29. The influence of the strips width on the von Misses stress for passive layer

3.2. The influence of the helix turns number

For every combination of materials, the helical winding angle has been changed (T={4π, 8π, 16π} which corresponds to a helix with 2, 4 and 8 turns), while the strips width has been maintained constant (b=10 mm). The numerical values for maximum deflection (ΔL [mm]), for the von Misses stress on the active layer (σ_{ea} [MPa]), as well as for the passive layer (σ_{ep} [MPa]) are presented in figures 30, 31, 32.

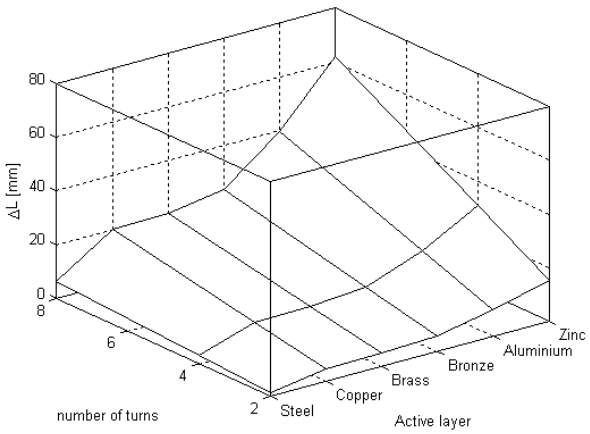

Fig. 30. The influence of the helix turns number on the maximum deflection

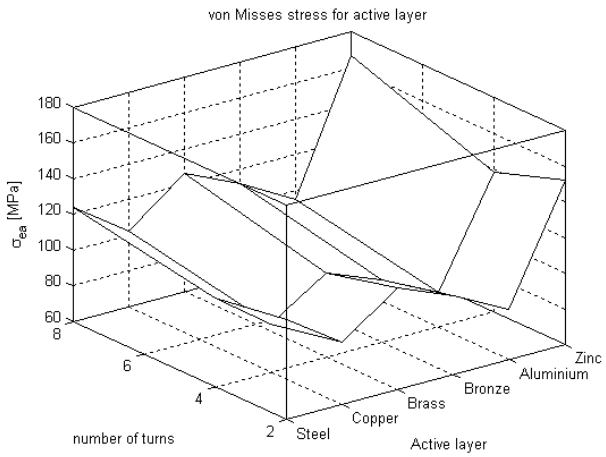

Fig. 31. The influence of the helix turns number on the von Misses stress for active layer

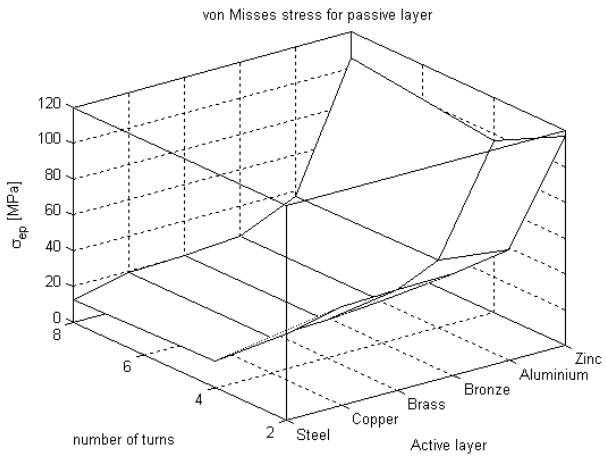

Fig. 32. The influence of the helix turns number on the von Misses stress for passive layer

4. CONCLUSIONS

The mesh parameters (the geometric parameters: size and sag, and the finite element type: linear or parabolic) have a great influence on the numerical analysis precision. For all the discretized 3D models with linear finite elements the global errors are in the range 22%...25%, which is an unacceptable error level. The linear finite element mesh could be improved by reducing the values of the size and sag parameters. Even if the adaptive mesh modifying method will be used, in order to decrease the global error it will be necessary to increase the number of mesh nodes and elements at very high levels. A better solution can be obtained if the parabolic finite element will be used (figures 7, 10 and 12). For the start global parameters, for all the discretized 3D models with parabolic finite elements the global errors are around the value of 20%, that is more closely of the desired error level (≈10%). The adaptive method for improving the mesh has been used for all helical bimetallic strips analysed. The adaptive mesh refinement has been performed in only one stage, from 20.81% to 8.34% for the helical bimaterial strip with p=50 mm (figure 9), from 20.74% to 7.85% for the helical bimaterial strip with p=25 mm (figure 11) and from 20.12% to 7.61% for the helical bimaterial strip with p=12.5 mm (figure 13). For all the improved meshes obtained by the adaptive method, a mesh refinement process has been automatically performed on the critical areas of the helical bimetallic strip elements in order to minimize the global error rate. The computing time has been increased from less than 1 minute (starting mesh with linear finite elements) to more than 5 minutes (improved mesh with parabolic finite elements). All computations have been performed on an AMD Athlon 64X2 Dual 3800+ at 2GHz processor with 2 GB RAM and 140 GB HDD. Decreasing the global error objective under 10% or decreasing the mesh parameters size and sag under certain levels can produce more often the computer freeze than the completed analysis.

All figures representing the displacements and the von Misses stress have an amplification magnitude of 1, corresponding thus to the reality. The study case presented in chapter 2 coresspond to titanium-zinc materials combination.

For all the study cases analyzed, the maximum von Misses stress can be observed in the clamped area (figures 16, 20 and 24). Another critical area, in terms of equivalent stress, is the interaction area between the two active and passive layers of the bimaterial helical temperature sensitive device (figures 17, 18; 21, 22 and 25, 25).

The width of the helical strips has a negligible influence on the maximum deflection (figure 27) for all combination of materials. As for the influence of the width of the helical strips on the streses, it becomes apparent that with width increasing, the von Misses stress grow as well but more visible in the active layer (figure 28) than in the passive layer (figure 29). For the case of zinc active layer the admissible strength is overcoming, thus a better design of the clamped area being necessary.

The helix turns number is definitely affects the values of the maximum deflection, increasing the number of turns, the deflection will increase ae well (figure 30). For all the study cases analyzed the von Misses stress in active layer is greater than in the passive layer (figures 31 and 32). The same conclusion can be observed on the width of the helical strips influence study (figures 28 and 29). The best combination of materials from the point of view of maximum deflection is titanium for passive layer and zinc for the active layer. Due to the smaller mechanical resistance of aluminium and zinc, increasing then width of the helical strips over a certain limit becomes dangerous, especially for the case of an accidental temperature increasing. An important conclusion has been made observing the graphical representation of the numerical analysis results even for an amplification magnitude of 1 (better view with an increased value), but also from the animation of the discretized model deformation. During the influence of the external temperature field the helical bimetallic strip will be deformed not only in the θ cylindrical axis direction, but also in the other two cylindrical axis directions, especially in the r cylindrical axis direction. The deformation in the θ axis direction represents the positive aspect, but the other deformations can be considered as negative aspects. The deformation in the r axis direction will change the helical shape of the temperature sensitive device, which has been considered to be a cylindrical helix before the deformation and will become a conical helix after the deformation.

5. REFERENCES

1. Ghionea, I.G. (2007). *Proiectare asistată în CATIA V5-Elemente teoretice şi aplicaţii*, BREN Publishing House, ISBN 978-973-648-654-8, Bucureşti.

2. Kanthal, AB. (2008). *Thermostatic Bimetal Handbook*, Available from: www.kanthal.com. Accessed: 7.01.2011.

3. Sandberg, R.J., (2000). *Temperature Measurement*, CRC Press. Available from: http://riyanto04.files.wordpress.com/2009/09/ch32.pdf. Accessed: 7.01.2011.

4. Zahariea, D., Stachie, M. (2010). *Structural Analysis of a Bimetallic Strip Thermostat*. Buletinul Institutului Politehnic din Iaşi, Tom LVI (LX), Fasc. 2, Secţia Construcţii de Maşini, ISSN 1011-2855, pp. 221-226.

5. Zamani, N.G. (2005). *CATIA V5-FEA Tutorials*, SDC Publications, ISBN 1-58503-259-X.

Received: February 09, 2011 / Accepted: May 30, 2011 / Paper published online: June 10, 2011